





Identification of Neurodegenerative Diseases From Gait Rhythm Through Time Domain and Time-Dependent Spectral Descriptors

Alessandro Mengarelli , Member, IEEE, Andrea Tigrini , Member, IEEE, Sandro Fioretti , and Federica Verdini 

Abstract—The analysis of gait rhythm by pattern recognition can support the state-of-the-art clinical methods for the identification of neurodegenerative diseases (NDD). In this study, we investigated the use of time domain (TD) and time-dependent spectral features (PSDTD) for detecting NDD sub-types. Also, we proposed two classification pathways for supporting NDD diagnosis, the first one made by a two-step learning phase, whereas the second one encompasses a single learning model. We considered stride-to-stride fluctuation data of healthy controls (CN), patients affected by Parkinson’s disease (PD), Huntington’s disease (HD), and amyotrophic lateral sclerosis (AS). TD feature set provided good results to distinguish between CN and NDDs, while performances lowered for specific NDD identification. PSDTD features boosted the accuracy of each binary identification task. With k -nearest neighbor classifier, the first diagnosis pathway reached 98.76% accuracy to distinguish between CN and NDD and 94.56% accuracy for NDDs sub-types, whereas the second pathway offered an overall accuracy of 94.84% for a 4-class classification task. Outcomes of this study indicate that the use of TD and PSDTD features, simple to extract and with a low computational load, provides reliable results in terms of NDD identification, being also useful for the development of gait rhythm computer-aided NDD detection systems.

Index Terms—Gait dynamics, neurological disorders, features extraction, pattern recognition, computer-aided diagnosis.

I. INTRODUCTION

NEURODEGENERATIVE diseases (NDD) represent a wide spectrum of disorders related to the impairment of neurological structures and manifest themselves with a variety of symptoms, leading to the decline of cognitive and physical capabilities [1]. Parkinson’s disease (PD) is the second most

common NDD, with a prevalence ranging from 100 to 200 per 100,000 people [2]. PD causes an altered output of the basal ganglia, and leads to hypokinetic movements, tremor, bradykinesia, rigidity, freezing of gait, and in general motor instability [1]. Huntington’s disease (HD) results from a selective loss of striatal neurons [1], and its most common symptoms are hyperkinetic limb and trunk movements, known as chorea, affecting almost 3 per 100,000 people [2]. Amyotrophic lateral sclerosis (AS) arises from the damage of the motor neurons innervating muscle fibers and motor control centers, with an impaired ability to regulate muscles’ activity, and it has a prevalence of 5 per 100,000 people [1], [2].

All the above mentioned NDDs share a degraded motor regulation and movement abnormalities, which are among the major factors leading to the risk of physical injuries and affecting daily life quality [1], [3]. Due to their degenerative nature, a reliable identification of these types of diseases is paramount in order to timely design and develop clinical treatment strategies [1], [4]. Currently, neuroimaging, magnetic resonance, computerized tomography, blood tests, and tissue biopsy are state of the art for NDD diagnosis [3], [5]. However, the clinical assessment based on these methods presents some drawbacks, being highly expensive, time-consuming, and invasive for the patient, requiring also expert personnel [2], [3], [5], [6]. Furthermore, in some cases, such techniques can provide poor results in terms of diagnostic reliability, as the case of magnetic resonance [6] and in general the misdiagnosis still remains a problem when dealing with NDD. For instance, up to 25% of PD diagnosis are incorrect [2], [6], since PD and HD patients present similar characteristics as the disease progresses and also AS may share clinical signs with PD [1], [2]. Hence, all these aspects support the investigation of alternative and reliable tools for assisting NDDs diagnosis, which should be in general also non-invasive, low-cost, and without the need for specific skills [4], [7], [8].

Human walking encompasses a series of periodic movements which involve the whole lower limb and gait abnormalities are commonly associated with NDDs [1]. Gait dynamics is typically quantified by spatial-temporal metrics, such as stride length, stride time, and speed, but their alterations were reported to be consistent among different diseases and thus do not distinguish specific NDD sub-types [1]. Conversely, the seminal works by Hausdorff and colleagues indicated that stride-to-stride

Manuscript received 17 December 2021; revised 22 April 2022 and 27 July 2022; accepted 4 September 2022. Date of publication 8 September 2022; date of current version 6 December 2022. (Alessandro Mengarelli and Andrea Tigrini are co-first authors.) (Corresponding author: Alessandro Mengarelli.)

The authors are with the Department of Information Engineering, Università Politecnica delle Marche, 60131 Ancona, Italy (e-mail: a.mengarelli@pm.univpm.it; a.tigrini@staff.univpm.it; s.fioretti@staff.univpm.it; f.verdini@staff.univpm.it).

This article has supplementary downloadable material available at <https://doi.org/10.1109/JBHI.2022.3205058>, provided by the authors.

Digital Object Identifier 10.1109/JBHI.2022.3205058

variability is a significant marker of gait alterations due to NDD [9], [10] and that stride-to-stride fluctuations are far to be noise, conveying instead information on non-linear dynamics of walking, which can be used to gain insights about the neural control of the motor system [1].

In the past few years, a growing amount of research investigated how NDDs affect specific properties of gait. Statistical-based analyses gave valuable information for describing walking dynamics in NDD individuals and highlighted significant differences in walking patterns of PD, HD, and AS patients [11], [12]. On the other hand, several studies followed a pattern recognition approach, in an attempt to develop computer-aided methodologies for the automatic detection of NDDs from gait signals, suited to support clinicians in the diagnostic and intervention phases.

Due to its prevalence, some studies focused on PD detection only, by using non-linear measures on stride-to-stride timeseries [13] or extracting features related to local changes from ground reaction force (GRF) [14]. However, an even more challenging issue is to succeed at correctly identifying an individual as healthy or suffering from a specific NDD. To accomplish this task, Baratin et al. [15] investigated the discrete wavelet transform (DWT), performing a series of linear binary classifications. The DWT was used also in [16], where attention was given to the recognition of AS with respect to PD, HS, and controls. On the other hand, features related to repeatability and complexity of gait timeseries were also investigated. The auto-correlation decay time, with the stride time and the fluctuation variation, was used in [7] for developing a wearable NDD detection system. The effectiveness of the Shannon entropy and statistical descriptors was evaluated in [17], whereas the conditional entropy, together with a phase synchronization analysis, based on the Hilbert transform, was employed in [18]. The use of texture-based features was investigated in [19], by using the fuzzy recurrence plot for converting gait timeseries into grayscale images. In [20] a feature set was built by fuzzy entropy, Lempel-Ziv complexity, and Teager-Kaiser operator, whereas Prabhu et al. [21] examined the classification performances of the recurrence quantification analysis (RQA). In [2] a non-negative least square coding algorithm, fed by the approximate entropy and statistical features, was tested for identifying PD, HD, and AS from GRF signals. The same learning model was used in [5], where the symmetry of right and left stride intervals was investigated through geometrical distance metrics, and by Saljuqi and Ghaderyan [3], who extracted coefficients from a time-frequency representation of the stride signal. Additional studies focused on the most suitable learning architectures for NDD recognition. Deep learning methods, such as convolutional neural networks, were tested on GRF timeseries [22]. In [23], a fuzzy inference system, based on artificial neural network, was proposed, whereas Zeng and Wang [24] adopted a deterministic learning approach for identifying gait dynamics, approximated by radial basis function neural networks, and then used for distinguishing between healthy and diseased individuals.

Despite all the above mentioned studies showing promising results, in almost all cases a series of binary classification tasks

were investigated, i.e. healthy controls versus NDDs or between NDD sub-types. On one hand, this allowed to assess the significance of the proposed methodologies for unveiling different gait dynamics and providing NDD identification. On the other hand, this kind of approach is far from being suitable as a diagnostic tool in an actual clinical scenario, since when an unseen subject comes into play, the latter should be identified without the need for choosing among several binary classification models.

In any pattern recognition context, the features selection is crucial for achieving high and robust classification performances. In particular, time domain (TD) features offer several advantages, since they need limited processing efforts to be extracted, do not require in general data-dependent computational parameters, as for non-linear or complexity related features [25], [26], and have a low computational load, being thus particularly suitable for on-line applications, such as myoelectric motion recognition [27]. In the latter field, TD features found an extensive employment [28], [29], showing in many cases higher performances with respect to features belonging to other domains [30], [31], for classification tasks which often involve several classes [29], [32]. It is noteworthy that different features computed in TD and used in myoelectric pattern recognition have been also successfully employed for gait rhythm analysis [13], [17], [20], [21], [27], [31]. This kind of features proved to be effective for NDD identification or when employed to boost the performances of more complex feature sets [2], [20], [21], [33].

Moreover, in recent years, the use of time-dependent spectral features (PSDTD) has been proposed [34], [35], [36]. PSDTD features are still computed in TD but account for the spectral properties of a signal, thus conveying different kind of information while preserving the advantages of remaining in TD for computation, which represents an important aspect for the development of wearable and real-time systems for physical condition monitoring and detection [7], [8]. This motivates an analysis focused on the performances offered by TD and PSDTD features when used on gait rhythm data for achieving a reliable NDD detection and specific disease identification.

The aim of the present work was twofold. Firstly, we investigated the suitability of different TD feature sets, commonly used in the field of myoelectric pattern recognition, for the identification of neurodegenerative disease from gait rhythm timeseries. In this context, we also tested the additional value of considering time-dependent spectral features for improving NDD detection. For this goal, we analyzed walking data relative to healthy control subjects and to patients affected by PD, HD, and AS. Secondly, we proposed two classification pathways, which could support non invasive NDD diagnosis in an actual clinical scenario.

II. METHODOLOGY

A. Gait Dataset

For this study, a publicly available gait dataset collected by Hausdorff et al. [9], [10] was considered. Data consist of gait recordings of 64 subjects: 16 healthy controls (CN), 15 patients

affected by PD, 20 patients with HD, and 13 patients suffering from AS. Eligibility criterion was the capacity to walk for at least 5 minutes without any assistive device and medication use was not modified for the experimental sessions. None of the subject presented additional pathologies or comorbidities which might affect walking dynamics [9]. The degree of neurological impairment for PD group is measured by the Hoehn and Yahr score (average value 2.8 ± 0.9) and the total functional capacity measure for the HD group (6.9 ± 3.8). For the AS population, the severity of disease is assessed by the time (months) since diagnosis (18.3 ± 17.8). More detailed information is reported in [9], [10], [33].

Subjects were asked to walk along a 77 m hallway for 5 minutes at their self-selected pace, in order to minimize walking variability [9], and instrumented with force-sensitive insoles, that provided time-series of the force applied to the ground during gait, sampled at 300 Hz (resolution 12 bit). The insole used for recording gait temporal data were developed by using conductive polymer layer sensors as transducers. Two force sensitive resistors were placed within the shoe by taping them to an insole. The first sensor was located in correspondence of the toes and the metatarsals whereas the second one was located under the heel. Further details can be found in [37]. The dataset comprises four gait time measures, acquired bilaterally: stride interval, swing duration, double support duration, and stance duration. In this study, we consider stride time intervals for further analyses.

B. Data Pre-Processing

From each gait recording, the first 20 s were removed in order to avoid biases due to startup effects [9], [10]. According with the experimental setup, subjects had to turn around and keep to walk as they approached the end of the hallway [9]. This might lead to spurious data which should be removed [12]. In this study, we chose as a threshold the standard deviation (SD) of the stride time-series and marked as outliers those data samples which are above or below 2·SD the median value of the entire stride time-series. As in [12], the less strict choice of 3·SD did not allow to recognize some spurious data, corresponding to turning points and easily detectable by visual inspection. Then, we discarded the data points marked as outliers and they were replaced with the median value of the time-series.

C. Feature Extraction

An initial set of 15 TD features was computed. This feature set encompasses common metrics used also the myoelectric pattern recognition field [31]: mean amplitude value (MAV), integrated absolute value (IAV), waveform length (WL), zero crossing (ZC), Willison amplitude (WA), slope sign change (SSC), variance (VAR), root mean square value (RMS), square integral (SI), absolute value of the third, fourth, and fifth temporal moment (TRD, FRTH, and FFTH), 4th order autoregressive coefficients (AR), difference absolute mean value (DAMV), and difference absolute standard deviation value (DASDV). For a detailed explanation of feature computation, the reader can refer to [31]. Note that since gait rhythm time-series, unlike sEMG

signals, are not zero-mean signals, for ZC computation their average value was subtracted. In addition, SSC is equivalent to the signal turns count metric [13], and thus we used the same threshold for SSC computation (0.05 s).

Then, we split the 15 TD features into different sets to be tested on gait data. As an aggregation criterion, we relied on well-acknowledged feature sets, representing a standard benchmark in a field where TD features proved to be highly effective for classification and found widespread employment, i.e. myoelectric-based gesture recognition [32], [38]. Hence, among 11 of the most commonly used feature sets for sEMG-based gesture classification [32], those made by TD metrics were selected:

- Hudgins's feature set (HUDFS) [27]: MAV, WL, ZC, and SSC.
- Du's feature set (DUFS) [28]: WL, ZC, SSC, IAV, VAR, and WA.
- TD and AR coefficients feature set (TDARFS) [29]: MAV, WL, SSC, VAR, WA, ZC, and AR.

In addition, 6 PSDTD features were also considered, accounting for the power spectrum but still computed in TD [34], [35]. The first three features are based on the root squared of the zero, second, and fourth order moments (m_0 , m_2 , and m_4). The general form is given by:

$$m_n = \sum_{k=0}^{N-1} k^n P(k) \quad (1)$$

where n is the moment order, k is the frequency index, and $P(k)$ is the power spectral density. For m_0 , the Parseval's theorem holds, stating that the sum of the square of a function equals the sum of the square of its Fourier transform. Higher-order even moments are calculated by relying on a differentiation property of the Fourier transform, i.e. the n^{th} derivative in TD corresponds to the multiplication of the spectrum for k to the power of n [34]. According to [35], the first three PSDTD features were then obtained as:

$$f_1 = \log(m_0) \quad (2)$$

$$f_2 = \log(m_0 - m_2) \quad (3)$$

$$f_3 = \log(m_0 - m_4) \quad (4)$$

The additional three PSDTD features are the sparseness (f_4), the irregularity factor (f_5), and the waveform length ratio (f_6). The first one provides a measure of the amount of energy packed into only few components [34], [36] and can be computed as follows:

$$f_4 = \log \left(\frac{m_0}{\sqrt{(m_0 - m_2)} \cdot \sqrt{(m_0 - m_4)}} \right) \quad (5)$$

The irregularity factor is defined as the ratio between the number of upward zero crossing and the number of peaks and it represents a measure of the signal regularity, expressed in terms of its spectral moments [36]:

$$f_5 = \log \left(\frac{m_2}{\sqrt{m_0 \cdot m_4}} \right) \quad (6)$$

Eventually, the waveform length ratio represents the ratio between the WL of the first and second derivative. It is amplitude scaling invariant [35] and is given by:

$$f_6 = \log \left(\frac{\sum_{i=1}^{N-1} |\Delta x|}{\sum_{i=1}^{N-1} |\Delta^2 x|} \right) \quad (7)$$

where x represents the signal and Δx and $\Delta^2 x$ denote the first and second derivative for discrete-time signals.

D. Classification Task

In this study, we initially selected five classifiers: k -nearest neighbor (kNN), support vector machine (SVM), decision tree (DT), multiclass logistic regression (MLR), and random forest (RF). These algorithms represent common machine learning methods used for NDD identification from gait data and thus were selected in order to allow a direct comparison with previous works, where the same problem was faced [6], [13], [14], [20], [21], [33]. In addition, they proved to be effective with small datasets, as the case of the present study. A detailed overview of the selected models can be found in [39].

For SVM, we used the radial basis function kernel [20], [21], with the σ value chosen within the set $\{0.01-1.5\}$. For kNN we set the number of nearest neighbors as $k \in \{1, \dots, 5\}$. The tree growing algorithm was the CART method [39] and for RF the number of trees was selected from 5 to 10 [20]. For each classification task and classifier, parameters' selection was performed by trial-error procedure [20], [21], in order to reach the best classification accuracy.

For each classifier, we adopted three cross validation (CV) methods. The first one is the leave-one-out cross validation (LOOCV), where one observation is used for testing while the remaining observations are used for training. This procedure is repeated holding out one observation at a time for training, until each of them has been used once for testing. This CV is commonly employed when dealing with small datasets and it has been used in similar studies [13], [20], [21]. The second method is the k -fold CV, where the dataset is split into k folds of equal size and then the first fold is used for validation and the remaining $k - 1$ folds are used for training. The process is repeated k times until each fold is used for validation and the others for training. In this study we set $k = 5$. The third method is the random sub-sampling. For each run, a randomly selected 70% of the entire dataset was used for training and the remaining 30% for testing the classifiers [20]. Classification performances were quantified by using accuracy (ACC), precision (PRC), recall (RCL), and specificity (SPC).

E. Experimental Setup

In this study, we performed two experiments, each of them involving different feature sets and classification tasks.

1) *Experiment 1*: In the first experiment we tested the validity of TD feature sets for NDD identification by training the five classifiers (kNN, SVM, DT, MLR, and RF) using HUDFS, DUFS, and TDARFS (see Section II-C). We investigated all the possible binary classification tasks, including the differentiation

between control subjects and NDD patients. This represents a yet employed scheme when dealing with NDD gait patterns recognition, hence allowing a direct comparison with previous studies [15], [20], [21], [33]. In this experiment, LOOCV method was used.

2) *Experiment 2*: In the second experiment we investigated the value of adding time-dependent spectral features for NDD identification. The 6 PSDTD features were added to the initial 15 TD features (see Section II-C). Then, in order to reduce the number of classifiers, we followed the approach presented in [20]. The accuracy of each single feature in distinguish between CN and NDD was computed for the five classifiers (see Section II-D) and the two which showed the highest number of features with an accuracy $>90\%$ were retained for the subsequent steps. The features with a single accuracy $<90\%$ were removed from the initial feature set for both the selected classifiers.

For each binary classification task, a backward sequential feature selection (B-SFS) was applied in order to find reduced feature subsets. The B-SFS algorithm belongs to the category of wrapper methods, suitable when dimensionality is low [40]. These methods perform a greedy search where candidate feature sets are built iteratively, with the goal to enhance the performances of pre-selected classifiers. In brief, given a d -dimensional feature space $\Omega = \{f_1, \dots, f_d\}$, a Γ_0 set is initialized as $\Gamma_0 = \Omega$. Then, the B-SFS algorithm constructs $d - 1$ subsets, each of them made by all the features in Γ_0 except for one. The absent features within the subset with the highest classification accuracy is removed from Γ_0 and then the same procedure is iterated $d - 1$ times, until Γ_0 contains only one feature. The optimal feature subset is chosen as that with the highest accuracy and the fewest dimensionality. The B-SFS was run for both the selected classifiers, obtaining in this way 14 reduced feature subsets (2 classifiers \times 7 binary comparisons).

Here, we used LOOCV and 5-fold CV methods. This was motivated by comparison purposes, since from previous works, dealing with the same topic, did not emerge a clear preference for a specific CV scheme and each of them found an almost equivalent employment [3], [6], [14], [19], [21].

In addition to this binary classification scheme, in this experiment we proposed two NDD identification pathways, which could be used in actual diagnosis scenarios. The first diagnosis pathway (DP1) is made by two learning steps and was similar to that proposed by Xia et al. [20]. The first step is the classification of a subject as healthy or affected by NDD and the second one is the identification of the specific disease (PD, HD, and AS). This second step was faced as a multi-class classification problem.

The second diagnosis pathway (DP2) was intended to prevent the use of a cascade of different classifiers, by using a single recognition step. Here, we avoided the distinction between controls and NDD patients and each classifiers was trained and tested for multi-class identification, i.e. for distinguishing directly between CN, PD, HD, and AS. To the best of our knowledge, this kind of 4-class classification has not been performed in similar works investigating the same dataset, where binary comparisons between NDD sub-types or with healthy controls were favored [3], [5], [6], [12], [33].

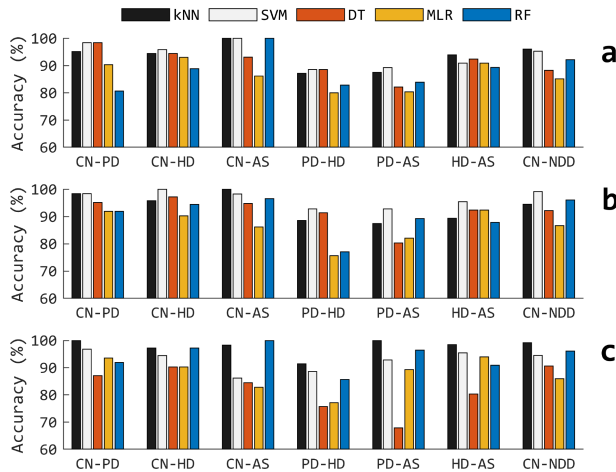


Fig. 1. Accuracy for the binary classification tasks for HUDFS (a), DUFS (b), and TDARFS (c) and for kNN, SVM, DT, MLR, and RF.

For multi-class tasks, i.e. distinguish between the three NDDs (DP1) and between all the groups (DP2), we built reduced feature sets as the union of the subsets obtained with the B-SFS. In the former case, we considered the subsets relative to the binary NDD classification tasks, while for the latter all the subsets were added up, i.e. including also those involving CN group. Finally, for both DP1 and DP2, we applied the random sub-sampling, performed over 50 runs, for cross validating the learning models. The average of the performance metrics computed over multiple runs was used for evaluating the goodness of the results. We selected this cross validation method in order to ease the comparison with [20], where a similar classification involving 4 groups was showed.

III. RESULTS AND DISCUSSION

A. Experiment 1

The classification accuracy for HUDFS, DUFS, and TDARFS is reported in Fig. 1. In order to keep the paper short, we reported the other metrics as supplementary material. Each TD feature set showed satisfying results for differentiating between controls and patients. DUFS provided the highest accuracy, averaged over all the classifiers, for the CN-PD (95.16%), CN-HD (95.56%), CN-AS (95.17%), and CN-NDD (93.75%), whereas a 100% accuracy was reached by the TDARFS (CN-PD with kNN) and DUFS (CN-HD with SVM). All the three feature sets gave 100% accuracy in distinguish between CN and AS groups, at least with one classifier. To be noted, this classification problem can be challenging, since it often reached low levels of accuracy compared with the other binary tasks [3], [15], [18], [20], [21].

DUFS and TDARFS showed good performances for CN-NDD classification, with 99.22% accuracy (SVM and kNN, Fig. 1). This accuracy is higher with respect to [20] and [15], where 96.83% and 80.4% were obtained with a larger feature set and DWT coefficients, respectively. Also data-driven features offered no superior performances for this task [6] and likewise if more refined learning schemes are considered, such as neuro-fuzzy inference [23] or deterministic learning [24].

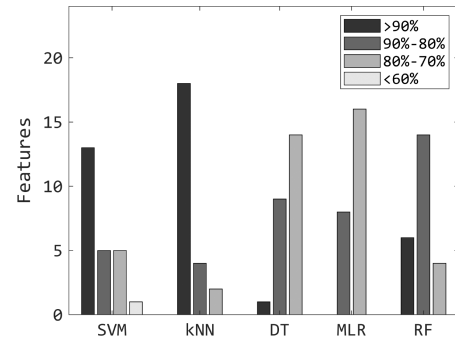


Fig. 2. Single feature accuracy for each considered classifier. The accuracy is computed for the CN-NDD classification task.

For the identification of NDD sub-types, each feature set showed a drop in the accuracy, more pronounced for the PD-HD case, resulting not higher than 93% (DUFS with the SVM, Fig. 1). The latter value is still higher than other studies [15], [17] but aligns with the work of Xia et al. [20], where this binary task showed the lowest accuracy among the others (91.18%). The TDARFS appears as the best feature set for PD-AS (100% accuracy) and HD-AS (98.49%) classification, both with kNN (Fig. 1), whereas HUDFS and DUFS failed to reach values beyond 94%, lower than those reported in previous studies [20], [21].

Overall, these results confirm that simple TD features are effective for gait rhythm data [33]. However, none of the feature sets provided stable accuracy levels, with a drop in distinguishing between NDD sub-types. Further, none of the learning methods showed performances comparable with those reported in previous studies, where in some [20], [33] or all [21] cases the accuracy resulted slightly higher. To be noted, in many studies [6], [20], [21] the optimal feature sets included metrics related to non-linear dynamics of timeseries, indicating the need for considering also features belonging to other domains. This supports our efforts for enhancing classification performances, made in the second experiment, by adding PSDTD features to the initial set.

B. Experiment 2

As reported in Fig. 2, kNN showed the highest number of single features with accuracy >90% (18), followed by SVM (13), and RF (6). Hence, for the next analyses we retained kNN and SVM. It is noteworthy that PSDTD features were 5 out of 18 for kNN and 4 out of 13 for SVM, supporting the value of spectral related features for this kind of problem. In the following, for multi-class problems, the one-versus-one method was employed for SVM [39].

Among the seven binary classification tasks (Table I), the kNN showed the best outcomes, reaching a 100% accuracy for all cases (LOOCV) and boosting the performances of the classical TD feature sets used in the first experiment. It is noteworthy that each optimal feature set, selected by the B-SFS algorithm, encompasses at least one PSDTD feature, pointing out the value of such kind of metrics. In addition, the MAV is the only feature shared with the HUDFS, DUFS, and TDARFS among the seven

TABLE I

CLASSIFICATION PERFORMANCE OF SVM AND kNN FOR ALL THE POSSIBLE BINARY CLASSIFICATION TASKS. RESULTS ARE RELATIVE TO THE LOOCV AND 5-FOLD CV METHODS

Classification	Classifier	ACC (%)		PRC (%)		RCL (%)		SPC (%)		Feature set
		LOOCV	5-FOLD	LOOCV	5-FOLD	LOOCV	5-FOLD	LOOCV	5-FOLD	
CN-PD	SVM	96.77	91.94	97.06	92.01	96.67	91.87	96.67	91.87	DAMV
	kNN	100	100	100	100	100	100	100	100	DAMV
CN-HD	SVM	100	97.22	100	97.62	100	96.88	100	96.88	f_4
	kNN	100	100	100	100	100	100	100	100	f_4
CN-AS	SVM	96.55	87.93	97.06	88.51	96.15	87.26	96.15	87.26	MAV, f_4
	kNN	100	100	100	100	100	100	100	100	f_4
PD-HD	SVM	97.14	94.29	97.62	95.45	96.67	93.33	96.67	93.33	DAMV, f_3
	kNN	100	97.14	100	97.62	100	96.67	100	96.67	f_2
PD-AS	SVM	100	100	100	100	100	100	100	100	SI, MAV, f_5
	kNN	100	100	100	100	100	100	100	100	DAMV, DASDV, f_5
HD-AS	SVM	96.97	93.94	97.62	95.45	96.15	92.31	96.15	92.31	MAV, f_5
	kNN	100	96.97	100	97.62	100	96.15	100	96.15	TRD, f_5
CN-NDD	SVM	100	96.88	100	98.00	100	93.75	100	93.75	IAV, DAMV, f_2
	kNN	100	98.44	100	97.06	100	98.96	100	98.96	DASDV, f_2

optimal sets (Table I), aligning with the role of this amplitude related metric for NDDs identification [20], [21], [33]. Further, TD features related to the derivative of the signal (DAMV and DASDV) turned out to be effective and the DAMV was in one case (CN-PD) sufficient to provide the best accuracy. Their role appears supported also by the findings reported in [9], [10], where the coefficient of variation and the SD of the detrended gait timeseries marked significant differences between controls and patients.

Results summarized in Table I represent a substantial advancement with respect to previous studies [6], [15], [18], [20] and improve what was reported by Prabhu et al. [21], who showed 100% accuracy for each binary comparison with RQA, except for CN-AS (96.15%), whereas we obtained 100% accuracy by using a single PSDTD feature. Outcomes appear to be promising also with respect to [3], where a 93%, 97%, and 94% accuracy was obtained (5-fold CV) by using linear and non-linear sparse decomposition-based features for identification of NDD sub-types with respect to controls.

It should be noted that in those studies where all the binary comparisons have been investigated, features related to non-linear dynamics of the gait timeseries were considered [17], [20], [21]. In both cases, it is required to set a series of computational parameters, such as the embedding dimension and the similarity threshold, which might result group-specific [41], being in general heavily data-dependent [25]. The features we investigated in this study do not rely on an *a priori* parameters' selection, combining high classification capabilities with significant advantages in terms of computational ease and direct applicability in practical scenarios [7], [8]. In this view, it is also remarkable that TD and PSDTD features are capable to offer the same performances of [19], where a 100% accuracy was reported for the CN-PD, CN-HD, and CN-AS cases (LOOCV). In the present work, we obtained the same results by relying on a single feature with a kNN classifier (Table I), whereas in [19] a total of 19 texture-based features were employed. Further, the extraction of texture-based features requires a preliminary conversion of the gait timeseries into images, by a fuzzy recurrence plot scheme,

limiting the possible usage of this method at a system level and for on-line applications.

Finally, the pattern recognition approach proposed in this study showed to be effective also if compared with previous works where more advanced classification methods were tested. Both SVM and kNN provided better outcomes with respect to the deterministic learning scheme proposed in [24] and to the adaptive neuro-fuzzy inference investigated by Ye et al. [23]. The former provided accuracy below 90% for each binary task involving CN group (LOOCV) and a 93.75% was obtained (all-training-all-testing) for the CN-NDD task. The latter obtained the best performance in distinguishing HD patients from the controls (94.44% accuracy, LOOCV), still lower than that provided by SVM and kNN by using also a single PSDTD feature (Table I).

For what concerns the DPI (Table II), both classifiers offered high performances in the first step, i.e. distinguishing between controls and NDD patients, also when the random sub-sampling CV is used instead of the LOOCV. A good level of accuracy was achieved also for the second step, i.e. the identification of specific NDD. The kNN confirmed to be the most suitable, also with higher RCL and SPC with respect to the SVM. Those metrics are of particular importance in clinical related applications, since they refer to the proportion of actual positive and negative cases correctly recognized.

The DPI appears thus a promising diagnosis tool for the NDD identification and this is supported also by the comparison with previous studies (Table IV). Using a set of simple statistical descriptors, Daliri [33] achieved 90.63% accuracy in the diagnosis of NDD, whereas for the same problem we obtained better results (Table II), also in terms of RCL and SPC in the case of kNN (98.86% versus 90.65% and 92.87%). The first step of DPI outperforms also the results presented in [6], where a 87.5% accuracy was obtained with data-driven features and DT classifier versus 98.76% of kNN, fed by only two features (Table II). With the same CV method, our two-step pathway outperformed also a similar diagnosis streamline proposed in [20]. On average, kNN provided over 99% of correctly recognized

TABLE II

CLASSIFICATION PERFORMANCE OF SVM AND KNN FOR THE DP1, WHERE A BINARY CLASSIFICATION IS FIRSTLY PERFORMED BETWEEN HEALTHY AND NDD SUBJECTS AND THEN SPECIFIC NDDs ARE RECOGNIZED BY A 3-CLASS CLASSIFIER. RESULTS ARE REPORTED AS THE AVERAGE OVER 50 RUNS OF THE RANDOM SUB-SAMPLING CROSS VALIDATION

Classification	Classifiers	ACC (%)	PRC (%)	RCL (%)	SPC (%)	Feature set
CN-NDD	SVM	95.20	97.01	90.24	90.24	IAV, DAMV, f_2
	kNN	98.76	97.93	98.86	98.86	DASDV, f_2
NDD	SVM	93.47	93.70	88.74	94.38	DAMV, SI, MAV, IAV, f_3, f_5
	kNN	94.56	91.89	91.91	95.84	DAMV, DASDV, TRD, f_2, f_5

TABLE III

CLASSIFICATION PERFORMANCE OF SVM AND KNN FOR THE DP2, WHERE A 4-CLASS CLASSIFICATION TASK IS PERFORMED. RESULTS ARE REPORTED AS THE AVERAGE OVER 50 RUNS OF THE RANDOM SUB-SAMPLING CROSS VALIDATION

Classification	Classifiers	ACC (%)	PRC (%)	RCL (%)	SPC (%)	Feature set
CN-PD-HD-AS	SVM	93.56	92.70	86.04	95.32	DAMV, SI, MAV, IAV, f_3, f_4, f_5
	kNN	94.84	89.98	89.53	96.49	DAMV, DASDV, TRD, f_2, f_4, f_5

TABLE IV

RECOGNITION PERFORMANCES (ACCURACY) FOR DIFFERENT NDD IDENTIFICATION DETECTION INVOLVING MACHINE LEARNING METHODS AND THE SAME TYPE OF CLASSIFICATION TASKS CONSIDERED IN THE PRESENT WORK. FOR MULTIPLE CLASSIFIERS, THE BEST CASE IS REPORTED

Work	Features	Classifiers	CN-PD	CN-HD	CN-AS	PD-HD	PD-AS	HD-AS	CN-NDD	NDD	ALL
[3]	Statistics, Non-linear	NNLS	93.0	97.0	94.0	-	-	-	-	-	-
[5]	Geometric distances	NNLS	98.0	95.0	97.0	-	-	-	-	-	-
[6]	Statistics, Correlation-based	DT	92.3	88.5	96.2	-	-	-	87.5	-	-
[15]	DWT coefficients	LDA	87.1	86.1	86.2	90.0	80.0	-	80.4	-	-
[17]	Statistics, Entropy	LDA	89.0	93.0	85.0	80.0	85.0	80.0	85.0	-	-
[18]	Phase synchronization	MLP, RF, NB	92.8	95.9	82.4	-	-	-	-	-	-
[19]	Texture-based	LS-SVM	100	100	100	-	-	-	-	-	-
[20]	Non-linear, Energy-based	SVM	100	100	96.6	91.2	96.4	96.9	96.8	-	-
[21]	RQA	SVM	100	100	96.2	100	100	100	-	-	-
[23]	Time intervals	ANFIS	90.3	94.4	93.1	-	-	-	90.63	-	-
[24]	Time intervals	DL	87.1	83.3	89.7	-	-	-	93.75	-	-
[33]	Statistics	SVM	89.3	90.3	96.8	-	-	-	90.6	-	-
Current work	TD, PSDTD	kNN, SVM	100	100	100	100	100	100	98.8	94.6	94.8

NNLS=Sparse non-negative least square coding, LDA=Linear discriminant analysis, MLP=Multilayer perceptron, NB = Naive Bayes, LS-SVM=Least square support vector machine, ANFIS=Adaptive neuro-fuzzy inference system, DL=Deterministic learning.

healthy subjects versus 93.67% and over 90% for PD, HD, and AS groups (Table V), whereas in [20] only for HD were achieved comparable results and in the other cases the correctly recognized patients remained below 85%.

With DP2, we investigated the feasibility of a single-step identification streamline, not yet proposed in similar studies (Table IV). Both kNN and SVM showed high identification performances, by using few features in each set (Table III). This confirms that the features selected by the B-SFS encompass significant information regarding the gait rhythm, valuable also within a multi-class framework. Note that both feature sets are made by 50% of PSDTD features, further emphasizing their crucial role for this kind of data.

The kNN showed overall better outcomes with respect to SVM, despite both models suffering from a relative lowering of the RCL if compared with DP1 (Table II). This is mirrored by the lower average percentage of the correctly recognized subjects for DP2 (Table V). The CN identification remains the most accurate, as for DP1, and comparable with that obtained in [20]. This could be linked to the highest number of samples available for training, but also to the fact that NDD patients could share some gait patterns, making easier their distinction

TABLE V

AVERAGE PERCENTAGE OF THE CORRECTLY RECOGNIZED SUBJECTS FOR THE TWO DIAGNOSIS PATHWAYS AFTER 50 RUNS OF THE RANDOM SUB-SAMPLING CROSS VALIDATION. RESULTS ARE RELATIVE TO THE KNN

Group	DP1 (%)	DP2 (%)
CN	99.06	92.54
PD	94.04	87.72
HD	90.72	90.19
AS	90.96	87.67

with respect to CN but more challenging for identifying NDD sub-types. Although, on the overall, DP2 resulted less accurate if compared to DP1 (Table V), it is still comparable with [20] for CN and HD classes (92.54% versus 93.67% and 90.19% versus 90.67%), while showed better performances in recognizing correctly PD and AS patients (87.72% versus 84.67% and 87.67% versus 81.50%). An overview of the results of the current work compared with some state-of-the-art studies is reported in Table IV. Eventually, it should be noted that, even if compared with deep learning schemes [22], the pattern recognition approach proposed in this study does not fail in

terms of classification performances (99.5% versus an average accuracy of 96.7% for DP1 and 94.4% for DP2), but preserves at the same time the clinical interpretability of the results, relying on features with a physiological meaning.

The main contributions of this work to existing literature can be summarized as follows: firstly, we investigated feature sets encompassing TD metrics not considered in previous studies for the identification of NDD from gait data, despite basic TD descriptors showing promising results for the same task [9], [12], [33]. Moreover, by considering PSDTD features, we assessed the value of spectral related information for NDD recognition, since the spectral properties of gait rhythm data have not been considered in past studies dealing with the same topic. Investigating PSDTD descriptors has an additional value in view of the development of a computer aided NDD identification system, since this kind of features preserves the advantages of being computed in time. Indeed, features in TD are extracted directly from raw data, without the need for any transformation, thus resulting efficient and cost-effective with respect to the computational load [31]. These are important requirements to fulfill for an actual hardware-level implementation [7], [8] and for on-line applications of pattern recognition approaches [34], [36], where incidentally the same kind of learning models adopted in this study are favored [35], [38] over more complex architectures [23], [24]. Thus, despite the evaluation of system-level aspects related to the technical development of a NDD identification device was beyond the scope of this study, our results can have a potential impact also in this area. However, additional studies are required to translate present findings into embedded technologies for motor functions and health assessment, where the challenge is to integrate software demands with hardware-level implementation [4], [7], [8].

A further contribution can be recognized in the two proposed diagnosis pathways, that can have beneficial impact on clinical implementation of NDD diagnosis, with the DP2 not presented in previous works (Table IV). In an actual application scenario, to an unseen subject it would be requested to perform a single walking trial and then the physician can use the DP1 in order to have support for the identification of the subject as healthy or affected by NDD and then for the diagnosis of the specific NDD. This requests to compute different features in each of the two stages, but with significant advantages in terms of accuracy and specificity of the diagnosis (Table II). If a faster screening is required, physician can rely on DP2, that offers the advantage of involving a single step of feature computation, providing a direct identification of the subject as healthy or affected by a specific NDD.

In both cases, good classification performances are combined with a high practical applicability, without the need for multiple binary comparisons. Each binary classifier has to be feed by different features and thus, in order to apply the proper learning model, binary classifications imply the prior knowledge of an unknown individual as belonging to a specific group, strongly hampering their practical clinical usage. Further, the identification result would be unreliable if the specific subject does not belong to the two groups for which the classifier was trained. Clinical applicability is also favored by considering that the proposed

NDD recognition architecture does not need instrumented environments for performing walking trials, since gait rhythm data can be easily recorded by force insoles or foot-switches [6], [37], [42], without the need for cumbersome and expensive recording systems. The easy requirements for data recording allow the proposed system also to be part of home-based solutions for health monitoring and disease diagnosis, since the patient does not need to be instrumented with obtrusive equipment, such as reflective markers and myoelectric probes. This can potentially impact on elderly people and on those unable to undergo to clinical screening on a regular basis, supporting at the same time remote clinical assessment.

Future studies should be devoted to collect datasets with a larger sample size and more refined levels of disease severity, in order to assess the value of TD and PSDTD descriptors for clinical evaluations about diseases development at different stages and for the design of therapeutic strategies. Further, the use of TD and PSDTD features might be investigated on different kind of gait data, such as ground reaction forces [2], [14], [22], without the need for raw data processing.

IV. CONCLUSION

Time-dependent spectral features alone resulted highly effective for the NDD recognition from gait data and PSDTD features appear to encompass significant information regarding the inner dynamics which regulate the temporal fluctuations of gait stride times. The diagnosis pathways proposed here proved to be effective for NDD identification within a multi-class framework, thus providing an additional perspective with respect to considering a series of binary classification tasks. The first pathway offered slightly superior performances with respect to the second one, which has not been proposed in previous studies but has instead the advantage of involving a single learning step. However, in both cases small feature sets (no more than 7 features) are needed for achieving high classification performances. All these aspects support the possible use of this kind of frameworks in actual scenarios, for automatic NDD gait pattern recognition, and for supporting clinical evaluations related to disease severity and progression.

REFERENCES

- [1] Y. Moon, J. Sung, R. An, M. E. Hernandez, and J. J. Sosnoff, "Gait variability in people with neurological disorders: A systematic review and meta-analysis," *Hum. Movement Sci.*, vol. 47, pp. 197–208, 2016.
- [2] S. M. G. Beyrami and P. Ghaderyan, "A robust, cost-effective and non-invasive computer-aided method for diagnosis three types of neurodegenerative diseases with gait signal analysis," *Measurement*, vol. 156, 2020, Art. no. 107579.
- [3] M. Saljuqi and P. Ghaderyan, "A novel method based on matching pursuit decomposition of gait signals for Parkinson's disease, Amyotrophic lateral sclerosis and Huntington's disease detection," *Neurosci. Lett.*, vol. 761, 2021, Art. no. 136107.
- [4] D. J. Cook, M. Schmitter-Edgecombe, L. Jönsson, and A. V. Morant, "Technology-enabled assessment of functional health," *IEEE Rev. Biomed. Eng.*, vol. 12, pp. 319–332, 2018.
- [5] P. Ghaderyan and S. M. G. Beyrami, "Neurodegenerative diseases detection using distance metrics and sparse coding: A new perspective on gait symmetric features," *Comput. Biol. Med.*, vol. 120, 2020, Art. no. 103736.
- [6] K. Gupta, A. Khajuria, N. Chatterjee, P. Joshi, and D. Joshi, "Rule based classification of neurodegenerative diseases using data driven gait features," *Health Technol.*, vol. 9, pp. 547–560, 2019.

- [7] W. Saadeh, M. A. B. Altaf, and S. A. Butt, "A wearable neuro-degenerative diseases detection system based on gait dynamics," in *Proc. IFIP/IEEE Int. Conf. Very Large Scale Integration*, 2017, pp. 1–6.
- [8] W. Saadeh, S. A. Butt, and M. A. B. Altaf, "A patient-specific single sensor IoT-based wearable fall prediction and detection system," *IEEE Trans. Neural Syst. Rehabil. Eng.*, vol. 27, no. 5, pp. 995–1003, May 2019.
- [9] J. M. Hausdorff, M. E. Cudkowicz, R. Firtion, J. Y. Wei, and A. L. Goldberger, "Gait variability and basal ganglia disorders: Stride-to-stride variations of gait cycle timing in Parkinson's disease and Huntington's disease," *Movement Disord.*, vol. 13, no. 3, pp. 428–437, 1998.
- [10] J. M. Hausdorff, A. Lertratanakul, M. E. Cudkowicz, A. L. Peterson, D. Kaliton, and A. L. Goldberger, "Dynamic markers of altered gait rhythm in amyotrophic lateral sclerosis," *J. Appl. Physiol.*, vol. 88, pp. 2045–2053, 2000.
- [11] A. Khajuria, P. Joshi, and D. Joshi, "Comprehensive statistical analysis of the gait parameters in neurodegenerative diseases," *Neurophysiology*, vol. 50, no. 1, pp. 38–51, 2018.
- [12] Y. Wu and S. Krishnan, "Statistical analysis of gait rhythm in patients with Parkinson's disease," *IEEE Trans. Neural Syst. Rehabil. Eng.*, vol. 18, no. 2, pp. 150–158, Apr. 2010.
- [13] Y. Wu et al., "Measuring signal fluctuations in gait rhythm time series of patients with Parkinson's disease using entropy parameters," *Biomed. Signal Process. Control*, vol. 31, pp. 265–271, 2017.
- [14] Ö. F. Ertuğrul, Y. Kaya, R. Tekin, and M. N. Almallı, "Detection of Parkinson's disease by shifted one dimensional local binary patterns from gait," *Expert Syst. Appl.*, vol. 56, pp. 156–163, 2016.
- [15] E. Baratin, L. Sugavaneswaran, K. Umopathy, C. Ioana, and S. Krishnan, "Wavelet-based characterization of gait signal for neurological abnormalities," *Gait Posture*, vol. 41, no. 2, pp. 634–639, 2015.
- [16] S. Bilgin, "The impact of feature extraction for the classification of amyotrophic lateral sclerosis among neurodegenerative diseases and healthy subjects," *Biomed. Signal Process. Control*, vol. 31, pp. 288–294, 2017.
- [17] S. Amin and A. Singhal, "Identification and classification of neuro-degenerative diseases using feature selection through PCA-LD," in *Proc. 4th IEEE Uttar Pradesh Sect. Int. Conf. Elect., Comput. Electron.*, 2017, pp. 578–586.
- [18] P. Ren, W. Zhao, Z. Zhao, M. L. Bringas-Vega, P. A. Valdes-Sosa, and K. M. Kendrick, "Analysis of gait rhythm fluctuations for neurodegenerative diseases by phase synchronization and conditional entropy," *IEEE Trans. Neural Syst. Rehabil. Eng.*, vol. 24, no. 2, pp. 291–299, Feb. 2016.
- [19] T. D. Pham, "Texture classification and visualization of time series of gait dynamics in patients with neuro-degenerative diseases," *IEEE Trans. Neural Syst. Rehabil. Eng.*, vol. 26, no. 1, pp. 188–196, Jan. 2018.
- [20] Y. Xia, Q. Gao, and Q. Ye, "Classification of gait rhythm signals between patients with neuro-degenerative diseases and normal subjects: Experiments with statistical features and different classification models," *Biomed. Signal Process. Control*, vol. 18, pp. 254–262, 2015.
- [21] P. Prabhu, A. K. Karunakar, H. Anitha, and N. Pradhan, "Classification of gait signals into different neurodegenerative diseases using statistical analysis and recurrence quantification analysis," *Pattern Recognit. Lett.*, vol. 139, pp. 10–16, 2020.
- [22] Z. Ning, L. Li, and X. Jin, "Classification of neurodegenerative diseases based on CNN and LSTM," in *Proc. 9th Int. Conf. Inf. Technol. Med. Educ.*, 2018, pp. 82–85.
- [23] Q. Ye, Y. Xia, and Z. Yao, "Classification of gait patterns in patients with neurodegenerative disease using adaptive neuro-fuzzy inference system," *Comput. Math. Methods Med.*, vol. 2018, 2018, Art. no. 9831252.
- [24] W. Zeng and C. Wang, "Classification of neurodegenerative diseases using gait dynamics via deterministic learning," *Inf. Sci.*, vol. 317, pp. 246–258, 2015.
- [25] H. Kantz and T. Schreiber, *Nonlinear Time Series Analysis*, vol. 7. Cambridge, U.K.: Cambridge Univ. Press, 2004.
- [26] A. Mengarelli, A. Tigrini, S. Fioretti, S. Cardarelli, and F. Verdini, "On the use of fuzzy and permutation entropy in hand gesture characterization from EMG signals: Parameters selection and comparison," *Appl. Sci.*, vol. 10, no. 20, 2020, Art. no. 7144.
- [27] B. Hudgins, P. Parker, and R. N. Scott, "A new strategy for multifunction myoelectric control," *IEEE Trans. Biomed. Eng.*, vol. 40, no. 1, pp. 82–94, Jan. 1993.
- [28] Y.-C. Du, C.-H. Lin, L.-Y. Shyu, and T. Chen, "Portable hand motion classifier for multi-channel surface electromyography recognition using grey relational analysis," *Expert Syst. Appl.*, vol. 37, no. 6, pp. 4283–4291, 2010.
- [29] H. Huang, H.-B. Xie, J.-Y. Guo, and H.-J. Chen, "Ant colony optimization-based feature selection method for surface electromyography signals classification," *Comput. Biol. Med.*, vol. 42, no. 1, pp. 30–38, 2012.
- [30] A. Tigrini, L. A. Pettinari, F. Verdini, S. Fioretti, and A. Mengarelli, "Shoulder motion intention detection through myoelectric pattern recognition," *IEEE Sens. Lett.*, vol. 5, no. 8, pp. 1–4, Aug. 2021.
- [31] A. Phinyomark, F. Quaine, S. Charbonnier, C. Serviere, F. Tarpin-Bernard, and Y. Laurillau, "EMG feature evaluation for improving myoelectric pattern recognition robustness," *Expert Syst. Appl.*, vol. 40, no. 12, pp. 4832–4840, 2013.
- [32] W. Wei, Q. Dai, Y. Wong, Y. Hu, M. Kankanhalli, and W. Geng, "Surface-electromyography-based gesture recognition by multi-view deep learning," *IEEE Trans. Biomed. Eng.*, vol. 66, no. 10, pp. 2964–2973, Oct. 2019.
- [33] M. R. Daliri, "Automatic diagnosis of neuro-degenerative diseases using gait dynamics," *Measurement*, vol. 45, no. 7, pp. 1729–1734, 2012.
- [34] R. N. Khushaba, A. Al-Ani, A. Al-Timemy, and A. Al-Jumaily, "A fusion of time-domain descriptors for improved myoelectric hand control," in *Proc. IEEE Symp. Ser. Comput. Intell.*, 2016, pp. 1–6.
- [35] A. H. Al-Timemy, R. N. Khushaba, G. Bugmann, and J. Escudero, "Improving the performance against force variation of EMG controlled multifunctional upper-limb prostheses for transradial amputees," *IEEE Trans. Neural Syst. Rehabil. Eng.*, vol. 24, no. 6, pp. 650–661, Jun. 2016.
- [36] R. N. Khushaba, M. Takruri, J. V. Miro, and S. Kodagoda, "Towards limb position invariant myoelectric pattern recognition using time-dependent spectral features," *Neural Netw.*, vol. 55, pp. 42–58, 2014.
- [37] J. M. Hausdorff, Z. Ladin, and J. Y. Wei, "Footswitch system for measurement of the temporal parameters of gait," *J. Biomech.*, vol. 28, no. 3, pp. 347–351, 1995.
- [38] R. N. Khushaba, E. Scheme, A. H. Al-Timemy, A. Phinyomark, A. Al-Tae, and A. Al-Jumaily, "A long short-term recurrent spatial-temporal fusion for myoelectric pattern recognition," *Expert Syst. Appl.*, vol. 178, 2021, Art. no. 114977.
- [39] J. Friedman et al., *The Elements of Stat. Learn.*, vol. 1. New York, NY, USA: Springer, 2001.
- [40] R. Kohavi and G. H. John, "Wrappers for feature subset selection," *Artif. Intell.*, vol. 97, no. 1-2, pp. 273–324, 1997.
- [41] A. Mengarelli, A. Tigrini, S. Fioretti, and F. Verdini, "Recurrence quantification analysis of gait rhythm in patients affected by Parkinson's disease," in *Proc. IEEE EMBS Int. Conf. Biomed. Health Inform.*, 2021, pp. 1–4.
- [42] F. Di Nardo et al., "EMG-based characterization of walking asymmetry in children with mild hemiplegic cerebral palsy," *Biosensors*, vol. 9, no. 3, 2019, Art. no. 82.